Observation of Peltier Cooling and Great Potential of Electroluminescent Cooling in GaN-Based Light-Emitting Diodes

Yiping Zhang, Shunpeng Lu, Baiquan Liu, Huayu Gao, Yubu Zhou, Wenhui Fang, Zi-Hui Zhang, Swee Tiam Tan, Hilmi Volkan Demir, and Xiao Wei Sun, *Fellow, IEEE*

***Abstract*— Light-emitting diodes (LEDs) are essential for future energy-saving lighting and display technology owing to their high efficiency, long lifetime, and low cost. To further enhance the performance of GaN-based LEDs, electroluminescent (EL) cooling has been widely predicted to be useful over the past several decades; however, it has not been experimentally achieved. Herein, thermoelectric and phonon-pumped GaN-based LEDs have been demonstrated by both experimental measurements and theoretical modeling. It is surprisingly found that the effect of increasing temperature changes from negative to positive when the operating point is moved to the high-efficiency, mid-voltage range. The power efficiency exhibits a maximum 2.24-fold improvement with increasing temperature (from room temperature to 473 K), and the peak efficiency at all elevated temperatures outperforms that at room temperature, where the Peltier effect changes from Peltier heat to Peltier cooling. Under lower biases, the phonon-assisted Peltier cooling provides additional energy for carriers to overcome the potential barrier and achieve recombination. The findings not only give an insightful understanding of EL cooling but also provide guidelines on thermal management and designing high-performance GaN-based LED devices and arrays (e.g., micro-LEDs), which can be further extended to other kinds of LEDs and optoelectronic devices.**

***Index Terms*— Electroluminescent (EL) cooling, GaN, light-emitting diode (LED), lighting, Peltier cooling.**

Received 14 January 2025; revised 21 May 2025 and 16 July 2025; accepted 22 July 2025. Date of publication 4 August 2025; date of current version 25 August 2025. This work was supported in part by Guangdong Basic and Applied Basic Research Foundation under Grant 2023B1515120046 and Grant 2024A0505090010; in part by the Program for Guangdong High-Level Talents under Grant 2021QN02X053; in part by Guangdong Innovation and Entrepreneurship Team Project under Grant 2021ZT09X070; in part by Singapore Agency for Science, Technology and Research (A*STAR) Science and Engineering Research Council (SERC) Pharos Program under Grant 1527300025; in part by the Collaborative Research in Engineering, Science and Technology Centre (CREST); and in part by Malaysia and Xiamen University Malaysia under Grant IENG/0039. The review of this article was arranged by Editor C.-C. Lin. *(Yiping Zhang, Shunpeng Lu, and Baiquan Liu contributed equally to this work.) (Corresponding authors: Baiquan Liu; Hilmi Volkan Demir.)*

Yiping Zhang and Hilmi Volkan Demir are with the Luminous! Centre of Excellence for Semiconductor Lighting and Displays, School of Electrical and Electronic Engineering, Nanyang Technological University, Singapore 639798 (e-mail: hvdemir@ntu.edu.sg).

Shunpeng Lu is with Changchun Institute of Optics, Fine Mechanics and Physics (CIOMP), Chinese Academy of Sciences (CAS), Changchun, Jilin 130033, China.

Baiquan Liu, Huayu Gao, Yubu Zhou, and Wenhui Fang are with the School of Electronics and Information Technology, Sun Yat-sen University, Guangzhou 510275, China (e-mail: liubq33@mail.sysu.edu.cn).

Zi-Hui Zhang is with the Luminous! Centre of Excellence for Semiconductor Lighting and Displays, School of Electrical and Electronic Engineering, Nanyang Technological University, Singapore 639798, and also with the School of Electronics and Information Engineering, Hebei University of Technology, Beichen, Tianjin 300401, China.

Swee Tiam Tan is with the Luminous! Centre of Excellence for Semiconductor Lighting and Displays, School of Electrical and Electronic Engineering, Nanyang Technological University, Singapore 639798, and also with the School of Energy and Chemical Engineering, Xiamen University Malaysia, Sunsuria, Selangor 43900, Malaysia.

Xiao Wei Sun is with the Institute of Nanoscience and Applications, Department of Electronic and Electrical Engineering, College of Engineering, Southern University of Science and Technology, Shenzhen 518055, China.

Digital Object Identifier 10.1109/TED.2025.3592917

I. Introduction

THE GaN-based light-emitting diodes (LEDs) are recognized as new-generation sources and become increasingly prevalent in lighting, display, and optical communication applications, owing to the great advantages in emission efficiency, lifetime, reliability, and cost [1], [2], [3]. Over the past decades, intense research and development efforts have been devoted to improve the performance of InGaN/GaN multiple quantum well (MQW) LEDs for their general lighting, micro-LED display, backlight sources, electronic equipment, and wireless communication applications [4], [5], [6], [7], [8], [9]. Most of them focus on the high-voltage bias regime of III-nitride MQW LEDs for which $qV > \hbar\omega$, where q is the elementary charge, V is the bias voltage, and $\hbar\omega$ is the average energy of an emitted photon [10], [11], [12]. To further enhance the performance of GaN-based LEDs, the phenomenon of electroluminescent (EL) cooling, which is a thermoelectric pumping process of carriers by electrical work and thermal energy obtained from phonon field via the Peltier effect, has been widely predicted to be useful over the past several decades. EL cooling is an extreme case of Peltier cooling, where the emitted photon energy is higher than the electrical input energy. In fact, EL cooling in semiconductor diodes was first reported by using a GaAs diode in 1964 [13]. Later, an experimental demonstration using an InGaAsSb infrared LED emitting at a wavelength of 2.42 μm was reported at elevated temperatures in 2012 [14], followed by several modeling and experiments reports on EL cooling

in GaAs-based light emitters by Sadi group [15], [16] and Santhanam group [17], [18].

In terms of GaN-based LEDs, some endeavors have been taken to understand EL cooling. For example, Piprek et al. [19] employed advanced device modeling to explore EL cooling in the GaN-based LEDs and theoretically proved the Peltier cooling from the numerical point of view. Hurni et al. [20] showed that the power efficiency of III-nitride LEDs could be greater than unity as a result of the energy absorption of carriers from phonon scattering. Xue et al. [21] later demonstrated the thermally enhanced GaN-based LEDs in a voltage region higher than 2.00 V through thermoelectric pumping. Recently, Sadi et al. [23] indicated the challenges of EL cooling in LEDs, and Kuritzky et al. [22] analyzed the prospects and possibilities of III-nitride LEDs for 100% power efficiency. Nevertheless, despite EL cooling being broadly predicted to be able to enhance the performance of LEDs for more than several decades, EL cooling has not been experimentally obtained or practically utilized in GaN-based LEDs so far. Furthermore, a comprehensive analysis and understanding of the temperature influence on the different operating regimes of LED devices is lacking, which is significantly required as the temperature affects the phonon field and may yield opposite effects on the LED performance in different bias regions.

In this work, we report thermoelectric and phonon-pumped GaN-based LEDs through both experimental measurements and numerical simulations. We show the influence of temperature on the power efficiency of blue-emission InGaN/GaN LEDs in three distinct voltage regions, where the effect of increasing temperature changes from negative to positive when the operating point is moved to the high-efficiency, midvoltage range. A maximum 2.24-fold improvement of power efficiency with increasing temperature over a large 175 K range (from room temperature to 473 K) and the peak power efficiency at all elevated temperatures outperforms that at room temperature with a maximum increment of 7.66%. In this region, the Peltier effect changes from Peltier heat to Peltier cooling, and the power efficiency is observed to be increased as the temperature rises, which is attributed to the increased carrier concentrations and stronger Peltier cooling. In the smaller bias region, the phonon-assisted Peltier cooling provides additional energy for carriers to overcome the potential barrier and achieve recombination, enhancing the power efficiency of blue-emitting InGaN/GaN LEDs. Raman measurements, together with the computation of total energy that carriers obtain from the phonon field, further support this observation. The temperature measurement of the LED device attached to the heat slug in the high vacuum chamber proves the capability of cooling down itself due to the Peltier cooling. To the best of our knowledge, this is not only the first report on the observation of EL cooling potential in GaN-based LEDs but also the experimental demonstration Peltier cooling in visible LEDs.

II. Experimental Section

The schematic of the InGaN/GaN MQWs LEDs used in this work and the schematic setup of the measurement are illustrated in Fig. 1, and the growth details of the wafers can be found in our previous work [24], [28]. After epitaxial growth,

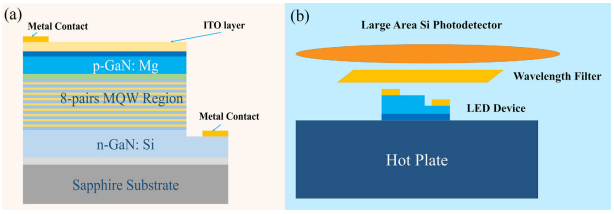

Fig. 1. (a) Schematic of the InGaN/GaN MQWs LED device. (b) Schematic of the experimental measurement setup.

the LED wafers were fabricated into devices with the dimensions of 1 × 1 mm using the standard fabrication processes. To achieve varied temperature conditions, the fabricated LED devices were placed on a hot plate and the optical output power was measured by a Si-photodiode, which was connected to the Thorlabs Dual Channel Optical Power and Energy Meter. During the measurements, the LEDs are driven by Keithley 6221, which has the capability to measure the current from pA to A. The electroluminescence wavelength is measured by an Ocean Optics Spectrometer attached to integrating sphere. The optical output power was measured by a Si photodiode (connected to the Thorlabs Dual Channel Optical Power and Energy Meter) with the lock-in technique. A Newport/Oriel 70680 Photomultiplier Tube together with Stanford Research Systems SR830 DSP Lock-in Amplifiers was used to further confirm that there is still some faint light from LED under low-voltage biases.

III. Results and Discussion

At present, one of the important problems associated with InGaN/GaN MQW LEDs is to improve thermal dissipation and avoid operating at elevated temperatures as the high temperature leads to thermal droop, degrading the device's power efficiency [24]. Due to this reason, a variety of cooling approaches are taken in III-nitride LEDs including modifying device architectures and providing external cooling designs to alleviate the thermal droop by reducing operating device temperature [25], [26], [27]. However, in contrast to the common knowledge and practice of operating InGaN/GaN LEDs, the increased device temperature may not necessarily lower the power efficiency under all conditions. Our hypothesis is that, when the operating voltage of InGaN/GaN LEDs falls into the midbias region of V photon voltage ($\hbar\omega/q$), the elevated temperature should become beneficial and enhance the device power efficiency, which is opposite to the temperature effect in the commonly known region of thermal droop, where the power efficiency rapidly drops with increasing bias and increasing temperature. Therefore, there must be different operating regions within which thermal heating may lead to completely opposite effects.

According to the well-known ABC model [28], internal quantum efficiency (IQE) can be expressed as follows at a low current injection level:

$$\mathrm{IQE} = Bn^2 \Big/ \left(An + Bn^2 + Cn^3\right) \tag{1}$$

where n is the carrier concentration, A is the Shockley–Read–Hall (SRH) nonradiative recombination rate, B is the radiative recombination rate, and C is the Auger nonradiative recombination rate. Under the low current injection level, the

SRH nonradiative recombination and radiative recombination are dominant compared to Auger nonradiative recombination. Then, the above equation is modified to [29]

$$\mathrm{IQE} = Bn^2 \Big/ \left(An + Bn^2\right). \tag{2}$$

The SRH nonradiative recombination has been reported to be increased with elevated temperature [30], [31], [32]; however, the carrier concentration is significantly increased with the temperature, as shown in the following equations, which may improve the IQE in one certain voltage region [14], [33]:

$$n^2 = n_i^2 \exp\left(\frac{qV}{kT}\right) \tag{3}$$

$$n_i^2 = N_c N_v \exp\left(\frac{-E_g}{kT}\right) = 2.33 \times 10^{31} \left(\frac{m_e^* m_h^*}{m_e^2}\right)^{3/2} T^3 \exp\left(\frac{-E_g}{kT}\right) \tag{4}$$

where n_i is the intrinsic concentration, q is the elementary charge, V is the applied voltage, k is the Boltzmann constant, T is the temperature, N_c is the effective density of states at conduction band edge, N_v is the effective density of states at the valence band edge, m_e^* is the effective electron mass, m_h^* is the effective hole mass, m_e is the free electron mass, and E_g is the energy bandgap of the material. From the above (2)–(4), it can be understood that for a low voltage when the device temperature is increased, the carrier concentration is considerably increased, which leads to the improved radiative recombination and possibly causes the enhanced IQE even though the SRH nonradiative recombination is simultaneously increased. In that case, the elevated temperature effect becomes beneficial when the applied voltage is small.

Fig. 2(a) presents the experimental optical output power and voltage curves versus the injection current for our InGaN/GaN LEDs at room temperature. For the voltages $V > \hbar\omega/q$, the applied voltage versus current follows a linear relationship, while for voltages $V < \hbar\omega/q$, the current is exponentially reduced with decreased voltage. From Fig. 2(b), the power efficiency reaches a maximum of 30.7% at 2.70 V ($V \approx \hbar\omega/q$) and then drops with the increase of applied voltage. The efficiency droop is about 36.9% when the voltage is increased from 2.70 to 4.00 V, which is due to the Auger recombination, the inhomogeneous carrier distribution, and the electron overflow [34]. Fig. 2(c) shows the EL spectral curves for our InGaN/GaN LEDs under varied voltage biases, where the peak emission remains the same for $V < \hbar\omega/q$. The peak is ~460 nm and slightly blue shift to 458 nm when the voltage is increased to 4.00 V [Fig. 2(d)], which is due to band-filling and charge screening effects under high carrier density [35].

Under the low-voltage condition [Fig. 2(b)], the power efficiency value is first decreased and then increased with a reduction in the applied voltage. It is well-known that conventional LEDs commonly show some light emission when the biased voltage is slightly lower than the photon voltage, but the power efficiency is low because the nonradiative recombination dominates. This phenomenon of current flow and light emission is possibly caused by carrier leakage through surface state or recombination assisted by deep levels [33]. Such

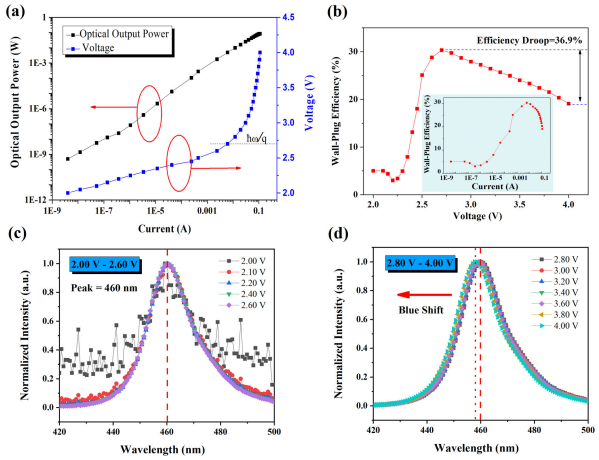

Fig. 2. (a) Optical output power and applied voltage versus injection current. (b) Power efficiency curve measured as a function of applied voltage; the inset shows the power efficiency curve versus the injected current. (c) EL spectral curves under different applied voltages from 2.00 to 2.60 V. (d) From 2.80 to 4.00 V for InGaN/GaN LEDs at room temperature.

mechanism may help but should not be dominant when the applied voltage is much lower than photon voltage, because the wavelength shifts, a phenomenon that is commonly observed when the deep-level-assisted recombination is involved [36], is not observed in the experimental measurements under the low-voltage condition [Fig. 2(c)]. More importantly, when it comes to the explanation of the slight enhancement of the power efficiency at the voltage around 2.00 V, this mechanism fails. Therefore, the radiative recombination at low voltages may be caused by another mechanism rather than the recombination at deep levels. A similar phenomenon of light emission at subphoton voltage is also observed in the recent work by Li et. al. [29] who reported the ultralow-power subphoton-voltage GaAs LEDs and indicated the possibility of net EL cooling, where the power efficiency is greater than unity. Thus, the light emission of InGaN/GaN LEDs in the low-voltage condition observed in the experiment is believed to be caused by Peltier cooling, which drives carriers to climb over the potential barrier and move forward into the active region.

To investigate the Peltier cooling, we measured the current–voltage (I–V) curves of the InGaN/GaN MQW LEDs at various temperatures tuned from 298 to 473 K [Fig. 3(a)]. It is worth noting that the turn-on voltage of the LEDs, which is the voltage required to have a significant current that can give a detectable brightness, is decreased from 2.40 to 2.20 V when the temperature is increased from 298 to 473 K, and the reduced turn-on voltage is ascribed to the thermoelectric pumping effect that continuously transfers excess thermal energy to carriers. Furthermore, the increased temperature causes a slight reduction in energy bandgap, further reducing the turn-on voltage [37]. Fig. 3(b) and (c) presents the experimental power efficiency curves and efficiency improvement versus the applied bias for our LEDs that are operated at different temperatures. The trend of the power efficiency in Fig. 3(b) is the same as the previous study of EL cooling reported for the InGaAsSb LED [14]. Fig. 3(c) shows that the influence of temperature on power efficiency varies in different operating regions separately by two inflection points: low-efficiency, low-voltage region ($V \leq 2.15$ V); high-efficiency,

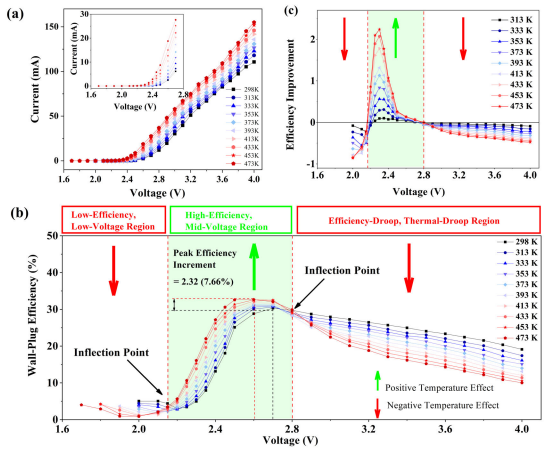

Fig. 3. (a) Experimental *I*–*V* curves for our InGaN/GaN LEDs measured at various temperatures; the inset shows the *I*–*V* curves at voltages lower than 2.70 V. (b) Experimentally measured power efficiency as a function of the applied bias across InGaN/GaN LEDs that were operated at systematically increased temperatures. (c) Relative power efficiency improvement at a certain temperature compared to the room temperature.

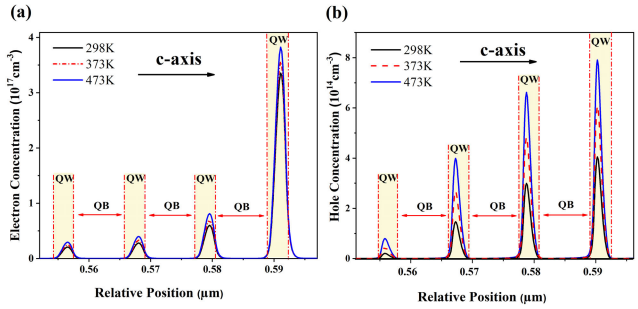

Fig. 4. (a) Numerically calculated electron concentration and (b) hole concentration in the last four QWs close to the p-GaN layer for the InGaN/GaN LEDs operated at a voltage of 2.40 V. Temperatures are set to 298, 373, and 473 K, respectively.

midvoltage region (2.15 V $< V <$ 2.85 V); and efficiency-droop, high-voltage region ($V \geq$ 2.85 V).

In the efficiency-droop, high-voltage region ($V \geq$ 2.85 V), with the increased applied bias, power efficiency begins to drop at all temperatures, known as the efficiency droop, which is believed to be caused by the high-carriers loss mechanisms, including carrier overflow, increased nonradiative recombination [38], and Auger recombination [34]. Operating in the high-efficiency, mid-voltage region (2.15–2.85 V), with increasing voltage, the power efficiency curves exhibit peculiar behavior: the power efficiency first increases and then declines after reaching a maximum value. In this region, the Peltier effect turns from Peltier heat to Peltier cooling as the voltage becomes lower than photon voltage, according to the approximated equation of the Peltier heat [21]

$$Q_{\text{Peltier heat}} = \left(V - IR - \frac{\hbar\omega}{q}\right) \times J \tag{5}$$

where J is the injection current density and R is the total series resistance of LEDs. Furthermore, the power efficiency is increasing at all bias points when the temperature is rising. As shown in Fig. 3(c), the power efficiency is improved by 2.24 folds for 2.30 V when the temperature is increased from 298 to 473 K. More importantly, the peak power efficiency at elevated temperatures outperforms that at room temperature and the maximum increment is 2.32% (7.66% in terms of improvement percentage), as marked in Fig. 3(b). This enhanced power efficiency is mainly attributed to the positive effect of increased temperature on carrier concentrations as indicated in (4) and enhanced Peltier cooling [21]. As the recombination mainly comes from the QWs close to the p-GaN region, Fig. 4 shows the calculated electron and hole concentrations in the last four QWs of the InGaN/GaN LEDs at 2.40 V, which indicates that both the electron and hole concentration are increased with the increasing temperature, which leads to improved power efficiency.

Finally, in the low-efficiency, low-voltage region ($V \leq$ 2.15 V), the power efficiency is found to be first decreased and then increased with the reduction of the applied voltage at different temperatures when the power efficiency levels are all low. In the low-bias regime, the external quantum efficiency (η_{EQE}) is observed to become independent of current [14]; thus, the power efficiency ($\eta_{\text{power}} = \eta_{\text{EQE}} * (\hbar\omega/V)$) is increased with the reduction of voltage. Moreover, with the increased temperature, the power efficiency is found to be reduced in this region. In this situation, the improved carrier concentrations caused by the increased temperature remain, but the effectiveness is limited due to the low value of the whole carrier concentrations and the great potential barrier the carriers encounter. It should be pointed out that, at different temperatures, the minimum applied voltage that can produce the detectable optical power is different for the tested devices since the available phonons are limited during the ballistic collisions and the number of phonons involved in Peltier heat exchange is varied. As indicated in Fig. 3(b), in the low-efficiency, low-voltage region, the LED power efficiency decreases with the increasing temperature, which is attributed to increased nonradiative recombination [31], the stronger quantum-confined Stark effect (QCSE) in QWs, and increased potential barrier in the AlGaN electron-blocking layer (EBL) [39], [40]. It is worth noting that the power efficiency of our device in this work is not high enough, which is mainly caused by nonoptimization device packaging and the limitation of the measurement methods, but the findings are consistent with previous reports [22], [23].

To further support this claim that the light emission of InGaN/GaN LEDs under low voltage is mainly attributed to the Peltier cooling, the numerical calculations were performed to compute the number of phonons needed to overcome the potential barrier (2.40 eV) for a certain applied voltage. Thus, the carriers need to absorb excess energy from the phonon field when the LED is driven by a voltage lower than the turn-on voltage. The total energy that the carriers may absorb should be larger than the energy needed coming from the difference between the potential barrier height and the applied bias.

In order to calculate the number of active phonons and how much energy these phonons are able to provide, Raman shift measurement for InGaN/GaN LED wafers at room temperature was carried out, and the experimental result is presented in Fig. 5. As indicated in Fig. 5(a), there are two main LO phonon modes in GaN: E mode and A mode with the corresponding wavenumbers of 572 and 737 cm^{-1}, respectively. The phonon number with frequency ω in GaN is

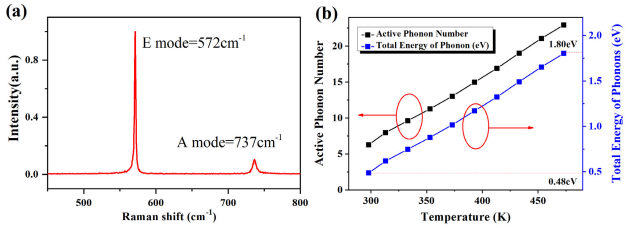

Fig. 5. (a) Raman shift of the InGaN/GaN LED that indicates two LO phonon modes: *E* mode and *A* mode. (b) Active phonon number and the energy that phonon field provides as a function of the temperature.

given by Bose–Einstein distribution function [13]

$$n_q = 1/\left(e^{\frac{\hbar\omega}{kT}} - 1\right) \tag{6}$$

where n_q is the phonon number with a certain frequency, $\hbar$ is the reduced Planck constant, ω is the frequencies of phonons, k is the Boltzmann constant, and T is the temperature.

To obtain the whole active phonon number for all modes at room temperature, we integrated the Raman shift curve in Fig. 5(a), as illustrated in the following equation:

$$n = \int_0^\infty n_q f(\omega) d\omega \tag{7}$$

where n is the total active phonon number for all modes and $f(\omega)$ is the Raman spectra curve. The temperature dependences of phonon frequency and linewidth were taken into consideration in the phonon number calculation for elevated temperature [42], [43], [44]. At room temperature, the active phonon number is found to be 6 and the total energy they are able to provide is around 0.48 eV [Fig. 5(b)]. Thus, as long as the applied bias is above 1.92 eV, the carriers still can overcome the potential barrier and move toward the active region by absorbing energy from the phonon field. This means that when the applied voltage is higher than 1.92 V ($2.40 - 0.48 = 1.92$), it is possible to observe light emission of the InGaN/GaN LEDs under such a low voltage at room temperature because the phonon field indeed provides enough energy for carriers. According to the experimental results in Fig. 3, the minimum voltage in which light emission can be experimentally detected is 2.00 V. This value is close to the theoretical calculations and the minor variation is probably because the power is too weak to be detected for $V < 2.00$ V. When the temperature is increased to 473 K, however, the active phonon number is substantially increased to 23 and the corresponding energy that can be provided by phonons rises to 1.80 eV. Thus, in principle, the minimum bias in which light emission assisted by the phonon field can be detected is 0.60 eV (0.60 V in terms of voltage), i.e., $2.40 - 1.80 = 0.60$. However, the minimum voltage that we can achieve experimentally is only 1.70 V. There are several limitations that prevent the measurements from further reaching such a low voltage. On the one hand, the optical output power for InGaN/GaN LEDs that are driven by the voltage of 1.70 V is about 7.6 nW, and a further reduction in the voltage leads to an extremely low optical power, which may be too weak to be detected. On the other hand, when the applied voltage keeps reducing, the required phonon number is also increasing. Particularly, when the voltage is reduced to as low as 0.60 V, 23 phonons are required to transfer their energy to one carrier all at once in order to overcome the potential barrier. Therefore, it is statistically difficult to achieve for the potential barrier for carriers to emission is quite high requiring 23 phonons to simultaneously transfer their energy to only one carrier. Thus, it can be concluded that Peltier cooling contributes to the light emission in the low-voltage range ($V < \hbar\omega/q$), but this observation for light emission assisted by Peltier cooling is difficult when the voltage is lower than 1.70 V for wide bandgap InGaN/GaN LEDs even less to achieve EL cooling the extreme case of the Peltier cooling. It is worth noting that the model used in this work to calculate the active phonon number and the total energy provided by the phonon field is a simplified one which may need further derivation. Considering that only small-wavevectored (close to Brillouin zone center) phonons are seen in the 1st-order (single phonon) Raman spectra and not all phonons are engaged in providing Peltier heat, the total active phonon number may be higher than that calculated by model and the exact energy provided by the phonon field may minorly vary, but this model still provides a possible method, in which phonons engage in Peltier heat.

To support that the reduction in minimum voltage from 2.00 to 1.70 V, in which light emission can be experimentally detected, is mainly caused by the improved phonon field and Peltier cooling rather than the variation in the energy bandgap, the numerical calculations on the variation in energy bandgap of GaN and InGaN layers are conducted. The temperature dependence of the energy bandgap of GaN and InN can be described by *Varshni* formula [45], as shown in the following:

$$E_g(T) = E_g(0) - \frac{\alpha T^2}{\beta + T} \tag{8}$$

where $E_g(T)$ is the energy bandgap at a certain temperature, $E_g(0)$ is the energy bandgap at 0 K, and α and β are the empirical constants. Thus, the variation of the energy bandgap in GaN and InN when the temperature is increased from room temperature to 473 K is given as

$$\Delta E_g(\Delta T) = \frac{\alpha T_0^2}{\beta + T_0} - \frac{\alpha T_1^2}{\beta + T_1}. \tag{9}$$

The energy bandgap of InGaN can be obtained from that of GaN and InN by *Vegard's* law [46], [47], as shown in the following:

$$E_g(\text{InGaN}) = E_g(\text{GaN}) * (1 - x) + E_g(\text{InN}) * x + bx(1 - x) \tag{10}$$

where x is the indium composition and b is the bowing parameter. In our case, the indium composition is about 18%. The values of bowing parameter, energy bandgap, and empirical constants of InN and GaN are taken from previous reports [46], [48]. We can get the variation of energy bandgap in GaN and InGaN due to the elevated temperature is −85.3 and −79.0 meV. Thus, the maximum reduction in the potential barrier caused by the decreased energy bandgap is 85.3 meV, which is smaller when band discontinuities are considered [49]. Thus, the reduction in minimum voltage observed in the experiment, which is 300 mV (300 meV in terms of energy), must be caused by the increased phonon field and enhanced Peltier cooling.

To further support that the InGaN/GaN device as a whole has the capability of cooling down itself, the LED die is encapsulated and attached to a large aluminum heat slug with

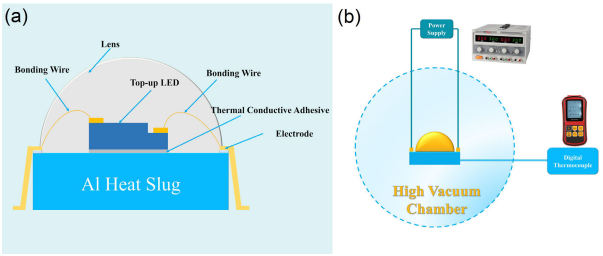

Fig. 6. (a) Schematic of the InGaN/GaN MQWs LED device with encapsulation attached with aluminum heat slug. (b) Schematic of the experimental setup of temperature measurement for the LED device hanging in the high vacuum chamber.

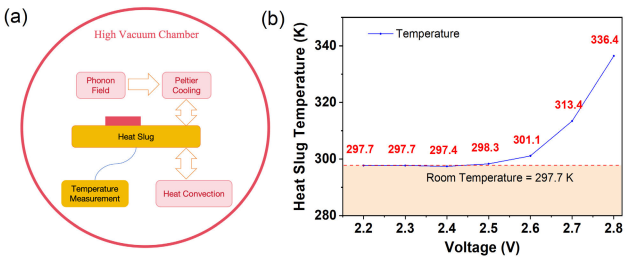

Fig. 7. (a) Schematic of thermal exchange for LED device in the high vacuum chamber. (b) Experimentally measured temperature of heat slug as a function of the applied voltage to the LED device.

a diameter and thickness of 6.0 and 1.0 mm, respectively. A digital thermocouple is attached to the aluminum heat slug for temperature measurement. Then, the total setup of the LED is allocated into a high vacuum chamber with a vacuum pressure of 4.05×10^{-7} mBar to reduce the air heat convection with the LED device and exclude the thermal noise from the environment. Two electrical wires for applying voltage also act as the mechanical connection to the LED device, so that the LED is hung by the wires without any other supports. Fig. 6(a) and (b) shows the schematic of the InGaN/GaN MQWs LED device with encapsulation attached with aluminum heat slug and the schematic of the experimental setup of temperature measurement for LED device hanging in the high vacuum chamber. As shown in Fig. 6(b), the LED device is driven by Keithley 6221 with pulsed measurement to reduce the thermal effects, and the temperature is measured by the digital thermocouple. The temperature measurement has been carried out in a scientific method and repeated several times, which ensures the accuracy of the measured results. Such a phenomenon can also be observed for different devices that further support the findings. Fig. 7(a) shows the schematic of thermal exchange for LED in the high vacuum chamber. In terms of the aluminum heat slug, its temperature is subjected to the coupling effect of thermal conduction with LED die and the air heat convection. Under low voltage, the thermal heat generated in the device is low, and if the Peltier cooling power of the LED die is greater than the heat convection, then the temperature of the heat slug will be reduced compared to its initial temperature and an increased one will be observed when the situation is reversed. Thus, according to Newton's law of cooling, for the heat slug, we have

$$\Delta Q = c * m * \Delta T = P_{\text{cool}} * A_{em} - P_{\text{heat convection}} * A \quad (11)$$

where ΔQ is the thermal heat variation, P_{cool} is the cooling power of the LED die under low voltage, $P_{\text{heat convection}}$ is the heat convection between the heat slug and air, A_{em} is the size of the LED die, A is the total surface area of the aluminum heat slug, through which the thermal heat is exchanged with the ambient, c is the heat capacity of the aluminum heat slug, m is the mass, and ΔT is the temperature variation of the heat slug compared to the initial temperature. According to the above equations, it can be seen that if the cooling power of the LED at low voltage is greater than the heat convection with the ambient, a reduced device temperature can be observed and a more dramatic temperature variation could be expected when the LED is allocated in a high vacuum chamber to reduce the air heat convection with the LED device.

As indicated in Fig. 7(b), the device temperature of InGaN/GaN LED is 297.5 K with a turn-on voltage of 2.40 V, 0.2 K lower than that of the LED without biases. For 2.40 V, the LED draws energy from the heat slug due to Peltier cooling, which results in a lowered temperature in the heat slug than its initial status. However, when the voltage is 2.60 V or even higher, a large amount of thermal heat is produced in the LED device, and thus, the heat slug temperature becomes much higher than the ambient temperature. In order to confirm the accuracy of the data obtained in the experiments, the measurement is repeated for multiple times. The voltage is first increased from 2.40 to 2.50 V, and the increased device temperature from 297.4 to 298.3 K is observed. Then, the applied voltage is reduced back to 2.40 V, and the device temperature measured is found to be reduced back to the previous value. The consistency in the device temperatures for different measurements indeed confirms the effectiveness of the experiments and the data accuracy in these experiments. Therefore, InGaN/GaN LEDs can cool down itself due to the Peltier cooling. Such findings are also expected to be applied for other optoelectronic devices [50].

IV. Conclusion

In conclusion, it is experimentally found that the Peltier cooling takes effect as the applied bias is reduced to lower biases ($V < \hbar\omega/q$). By absorbing energy from the phonon field, the carriers are able to overcome the potential barrier and make it to the QWs to radiate even when the applied bias is low. Computing the phonon number required for carriers to overcome the potential barrier and then comparing it to the active phonon number under various temperature conditions, the minimum bias voltage at which the LEDs can undergo Peltier cooling is found to be consistent with the minimum voltage at which LEDs are driven to produce the detectable optical signal. The temperature effects on the InGaN/GaN LEDs systematically analyzed and identified in different operating regions are found to be beneficial at elevated temperatures specifically in the high-efficiency, mid-voltage range. The conducted temperature measurement of the heat slug attached to the LED die further proves the capability of cooling down itself. The results not only unlock the potential of EL cooling for GaN-based LEDs but also provide guidelines on thermal management and sustaining high-performance GaN-based LEDs (e.g., LED arrays and micro-LEDs), which can be further extended to other kinds of LEDs (e.g., quantum dot LEDs, perovskite LEDs, and colloidal quantum well LEDs).

REFERENCES

[1] Y. Kobayashi, K. Kumakura, T. Akasaka, and T. Makimoto, "Layered boron nitride as a release layer for mechanical transfer of GaN-based devices," *Nature*, vol. 484, p. 223, Apr. 2012.

[2] N. Han et al., "Improved heat dissipation in gallium nitride light-emitting diodes with embedded graphene oxide pattern," *Nat. Commun.*, vol. 4, p. 1452, Feb. 2013.

[3] F. A. Ponce and D. P. Bour, "Nitride-based semiconductors for blue and green light-emitting devices," *Nature*, vol. 386, p. 351, Mar. 1997.

[4] S. T. Tan, X. W. Sun, H. V. Demir, and S. P. DenBaars, "Advances in the LED materials and architectures for energy-saving solid-state lighting toward 'lighting revolution,"' *IEEE Photon. J.*, vol. 4, no. 2, pp. 613–619, Apr. 2012.

[5] S. Pimputkar, J. S. Speck, S. P. DenBaars, and S. Nakamura, "Prospects for LED lighting," *Nature Photon.*, vol. 3, p. 180, Apr. 2009.

[6] T.-I. Kim et al., "Injectable, cellular-scale optoelectronics with applications for wireless optogenetics," *Science*, vol. 340, p. 211, Apr. 2013.

[7] B. Tang et al., "Enhanced light extraction of flip-chip mini-LEDs with prism-structured sidewall," *Nanomaterials*, vol. 9, p. 319, Feb. 2019.

[8] S.-I. Park et al., "Printed assemblies of inorganic light-emitting diodes for deformable and semitransparent displays," *Science*, vol. 325, p. 977, Aug. 2009.

[9] Y. Huang, E.-L. Hsiang, M.-Y. Deng, and S.-T. Wu, "Mini-LED, Micro-LED and OLED displays: Present status and future perspectives," *Light Sci. Appl.*, vol. 9, p. 105, Jun. 2020.

[10] S. Choi et al., "Improvement of peak quantum efficiency and efficiency droop in III-nitride visible light-emitting diodes with an InAlN electron-blocking layer," *Appl. Phys. Lett.*, vol. 96, May 2010, Art. no. 221105.

[11] Y. J. Lee, C. H. Chen, and C. J. Lee, "Reduction in the efficiency-droop effect of InGaN green light-emitting diodes using gradual quantum wells," *IEEE Photon. Technol. Lett.*, vol. 22, no. 20, pp. 1506–1508, Aug. 12, 2010.

[12] S. Tanaka et al., "Droop improvement in high current range on PSS-LEDs," *Electron. Lett.*, vol. 47, p. 335, Mar. 2011.

[13] G. C. Dousmanis, C. W. Mueller, H. Nelson, and K. G. Petzinger, "Evidence of refrigerating action by means of photon emission in semiconductor diodes," *Phys. Rev.*, vol. 133, p. A316, Jan. 1964.

[14] P. Santhanam, D. J. Gray, and R. J. Ram, "Thermoelectrically pumped light-emitting diodes operating above unity efficiency," *Phys. Rev. Lett.*, vol. 108, Mar. 2012, Art. no. 097403.

[15] T. Sadi, P. Kivisaari, J. Tiira, I. Radevici, T. Haggren, and J. Oksanen, "Electroluminescent cooling in intracavity light emitters: Modeling and experiments," *Opt. Quantum Electron.*, vol. 50, p. 18, Jan. 2017.

[16] I. Radevici et al., "Thermophotonic cooling in GaAs based light emitters," *Appl. Phys. Lett.*, vol. 114, Feb. 2019, Art. no. 051101.

[17] K. Chen, T. P. Xiao, P. Santhanam, E. Yablonovitch, and S. Fan, "High-performance near-field electroluminescent refrigeration device consisting of a GaAs light emitting diode and a Si photovoltaic cell," *J. Appl. Phys.*, vol. 122, no. 14, Oct. 2017, Art. no. 143104.

[18] T. P. Xiao, K. Chen, P. Santhanam, S. Fan, and E. Yablonovitch, "Electroluminescent refrigeration by ultra-efficient GaAs light-emitting diodes," *J. Appl. Phys.*, vol. 123, no. 17, May 2018, Art. no. 173104.

[19] J. Piprek and Z. Li, "Electroluminescent cooling mechanism in InGaN/GaN light-emitting diodes," *Opt. Quantum Electron.*, vol. 48, no. 10, p. 472, Sep. 2016.

[20] C. A. Hurni et al., "Bulk GaN flip-chip violet light-emitting diodes with optimized efficiency for high-power operation," *Appl. Phys. Lett.*, vol. 106, no. 3, Jan. 2015, Art. no. 031101.

[21] J. Xue et al., "Thermally enhanced blue light-emitting diode," *Appl. Phys. Lett.*, vol. 107, no. 12, Sep. 2015, Art. no. 121109.

[22] L. Y. Kuritzky, C. Weisbuch, and J. S. Speck, "Prospects for 100% wall-plug efficient III-nitride LEDs designed for low current density operation," *Opt. Exp.*, vol. 26, p. 16600, Sep. 2018.

[23] T. Sadi, I. Radevici, and J. Oksanen, "Thermophotonic cooling with light-emitting diodes," *Nature Photon.*, vol. 14, no. 4, pp. 205–214, Apr. 2020.

[24] B. Liu et al., "An ideal host-guest system to accomplish high-performance greenish yellow and hybrid white organic light-emitting diodes," *Organic Electron.*, vol. 27, pp. 29–34, Jan. 2015.

[25] R. H. Horng, C. C. Chiang, H. Y. Hsiao, X. Zheng, D. S. Wuu, and H. I. Lin, "Improved thermal management of GaN/sapphire light-emitting diodes embedded in reflective heat spreaders," *Appl. Phys. Lett.*, vol. 93, no. 11, Sep. 2008, Art. no. 111907.

[26] B. Sun et al., "Dislocation-induced thermal transport anisotropy in single-crystal group-III nitride films," *Nature Mater.*, vol. 18, no. 2, pp. 136–140, Feb. 2019.

[27] M. Kneissl, T.-Y. Seong, J. Han, and H. Amano, "Deep-ultraviolet light-emitting diodes based on AlGaN alloys," *Nature Photon.*, vol. 13, no. 4, pp. 233–241, Apr. 2019.

[28] Y. P. Zhang et al., "Nonradiative recombination–critical in choosing quantum well number for InGaN/GaN light-emitting diodes," *Opt. Exp.*, vol. 23, no. 3, pp. A34–A42, Jan. 2015.

[29] N. Li et al., "Ultra-low-power sub-photon-voltage high-efficiency light-emitting diodes," *Nature Photon.*, vol. 13, no. 9, pp. 588–592, Sep. 2019.

[30] D.-P. Han et al., "Nonradiative recombination mechanisms in InGaN/GaN-based light-emitting diodes investigated by temperature-dependent measurements," *Appl. Phys. Lett.*, vol. 104, no. 15, Apr. 2014, Art. no. 151108.

[31] M. I. Hossain, Y. Itokazu, S. Kuwaba, N. Kamata, and H. Hirayama, "Preparation and investigation of optical, structural, and morphological properties of nanostructured ZnO: Mn thin films," *Opt. Mater.*, vol. 105, Jun. 2020, Art. no. 109878.

[32] C. D. Santi et al., "Recombination mechanisms and thermal droop in AlGaN-based UV-B LEDs," *Photon. Res.*, vol. 5, no. 2, p. A44, Mar. 2017.

[33] E. F. Schubert, *Light-Emitting Diodes*, 2nd ed., Cambridge, U.K.: Cambridge Univ. Press, 2006.

[34] D. S. Meyaard et al., "Temperature dependent efficiency droop in GaInN light-emitting diodes with different current densities," *Appl. Phys. Lett.*, vol. 100, no. 8, Feb. 2012, Art. no. 081106.

[35] J. K. Sheu et al., "Luminescence of an InGaN/GaN multiple quantum wells light-emitting diode," *Solid-State Electron.*, vol. 44, no. 6, p. 1055, Jun. 2000.

[36] W. Grieshaber, E. F. Schubert, I. D. Goepfert, R. F. Karlicek, M. J. Schurman, and C. Tran, "Competition between band gap and yellow luminescence in GaN and its relevance for optoelectronic devices," *J. Appl. Phys.*, vol. 80, no. 12, pp. 4615–4620, Dec. 1996.

[37] Y. Cho et al., "'S-shaped' temperature-dependent emission shift and carrier dynamics in InGaN/GaN multiple quantum wells," *Appl. Phys. Lett.*, vol. 73, pp. 1370–1372, Sep. 1998.

[38] Q. Dai et al., "On the symmetry of efficiency-versus-carrier-concentration curves in GaInN/GaN light-emitting diodes and relation to droop-causing mechanisms," *Appl. Phys. Lett.*, vol. 98, no. 3, Jan. 2011, Art. no. 033506.

[39] O. Ambacher et al., "Pyroelectric properties of Al(In)GaN/GaN hetero- and quantum well structures," *J. Phys., Condens. Matter*, vol. 14, no. 13, pp. 3399–3434, Mar. 2002.

[40] W. S. Yan et al., "Temperature dependence of the pyroelectric coefficient and the spontaneous polarization of AlN," *Appl. Phys. Lett.*, vol. 90, May 2007, Art. no. 212102.

[41] G. Hansdah and B. K. Sahoo, "Pyroelectric effect and lattice thermal conductivity of InN/GaN heterostructure," *J. Phys. Chem. Solids*, vol. 117, p. 111, Jun. 2018.

[42] A. Link et al., "Temperature dependence of the E_2 and A_1(LO) phonons in GaN and AlN," *J. Appl. Phys.*, vol. 86, no. 11, pp. 6256–6260, Dec. 1999.

[43] M. S. Liu, L. A. Bursill, S. Prawer, K. W. Nugent, Y. Z. Tong, and G. Y. Zhang, "Conditioning nano-LEDs in arrays by laser-micro-annealing: The key to their performance improvement," *Appl. Phys. Lett.*, vol. 74, no. 19, p. 3125, May 1999.

[44] D. Y. Song et al., "The influence of phonons on the optical properties of GaN," *J. Appl. Phys.*, vol. 100, no. 11, Dec. 2006, Art. no. 113504.

[45] Y. P. Varshni, "Temperature dependence of the energy gap in semiconductors," *Physica*, vol. 34, no. 1, pp. 149–154, 1967.

[46] W. Walukiewicz et al., "Band gap engineering of dilute nitrides," *J. Cryst. Growth*, vol. 269, no. 1, pp. 119–125, Aug. 2004.

[47] H. M. Foronda et al., "Thermal stability and incorporation of er in GaN grown by metalorganic vapor phase epitaxy," *J. Cryst. Growth*, vol. 475, pp. 127–133, Oct. 2017.

[48] I. Vurgaftman and L. R. Ram-Mohan, "Band parameters for nitrogen-containing semiconductors," *J. Appl. Phys.*, vol. 89, pp. 5815–5875, Sep. 2001.

[49] G. Martin, A. Botchkarev, A. Rockett, and H. Morkoç, " Valence-band discontinuities of wurtzite GaN, AlN, and InN heterojunctions measured by x-ray photoemission spectroscopy," *Appl. Phys. Lett.*, vol. 68, no. 18, pp. 2541–2543, Apr. 1996.

[50] D. Luo, Y. Yang, L. Huang, B. Liu, and Y. Zhao, "High-performance hybrid white organic light-emitting diodes exploiting blue thermally activated delayed fluorescent dyes," *Dyes Pigments*, vol. 147, pp. 83–90, Dec. 2017.